The Use of Moisture Flux Convergence in Forecasting Convective Initiation: Historical and Operational Perspectives

PETER C. BANACOS

NOAA/NWS/NCEP/Storm Prediction Center, Norman, Oklahoma

DAVID M. SCHULTZ

Cooperative Institute for Mesoscale Meteorological Studies, University of Oklahoma, and NOAA/National Severe Storms Laboratory, Norman, Oklahoma

Weather and Forecasting

FORECASTER'S FORUM

Submitted: 26 October 2004

Revised: 21 December 2004

Corresponding author address: Peter C. Banacos, Storm Prediction Center, 1313 Halley Circle, Norman, OK 73069. E-mail: peter.banacos@noaa.gov

ABSTRACT

Moisture flux convergence (MFC) is a term in the conservation of water vapor equation and was first calculated in the 1950s and 1960s as a vertically integrated quantity to predict rainfall associated with synoptic-scale systems. Vertically integrated MFC was also incorporated into the Kuo cumulus parameterization scheme for the Tropics. MFC was eventually suggested for use in forecasting convective initiation in the midlatitudes in 1970, but practical MFC usage quickly evolved to include only surface data, owing to the higher spatial and temporal resolution of surface observations. Since then, surface MFC has been widely applied as a short-term (0–3 h) prognostic quantity for forecasting convective initiation, with an emphasis on determining the favorable spatial location(s) for such development.

A scale analysis shows that surface MFC is directly proportional to the horizontal mass convergence field, allowing MFC to be highly effective in highlighting mesoscale boundaries between different air masses near the Earth's surface that can be resolved by surface data and appropriate grid spacing in gridded analyses and numerical models. However, the effectiveness of boundaries in generating deep moist convection is influenced by many factors, including the depth of the vertical circulation along the boundary and the presence of convective available potential energy (CAPE) and convective inhibition (CIN) near the boundary. Moreover, lower- and upper-tropospheric jets, frontogenesis, and other forcing mechanisms may produce horizontal mass convergence above the surface, providing the necessary lift to bring elevated parcels to their level of free convection without connection to the boundary layer. Case examples elucidate these points as a context for applying horizontal mass convergence for convective initiation. Because horizontal mass convergence is a more appropriate diagnostic in

an ingredients-based methodology for forecasting convective initiation, its use is recommended over MFC.

1. Introduction

Convective initiation (CI) remains a difficult forecast challenge (e.g., Ziegler and Rasmussen 1998; Moller 2001). Predicting the precise timing and location of deep moist convection, even along well-defined surface boundaries (e.g., fronts, drylines), remains a hurdle to improved short-range forecasts of severe weather and has been the subject of recent field work such as 2002's International H2O Project (IHOP) (Weckwerth et al. 2004).

In view of imperfect scientific knowledge concerning processes related to CI, as well as inadequacies in numerical guidance concerning, in particular, warm-season convective storm evolution (Fritsch and Carbone 2004), forecasters have necessarily sought a variety of diagnostic measures to aid in forecasting CI using derived parameters from both observations and numerical model output. One such variable is moisture flux convergence (MFC). Reviews of the strengths and limitations of surface MFC have appeared in Doswell (1982), Bothwell (1988), and Waldstreicher (1989).

Evaluating the utility of forecasting techniques is one role of the daily map discussions between Storm Prediction Center (SPC) forecasters and National Severe Storms Laboratory (NSSL) researchers (e.g., Kain et al. 2003c). During one such map discussion, the role of surface MFC for predicting CI was questioned. Afterward, discussions amongst our two groups continued, leading to a more extensive evaluation of MFC, including a survey of the available scientific literature. Importantly, surface MFC was tested in the real-time operational setting of the SPC, noting its successes and failures. Because of our investigations, we believe we have discovered some hitherto underappreciated, and unappreciated, aspects of MFC.

The goals of this article are to: 1) trace the historical usage of MFC as a forecast tool to understand the physical rationale behind its origin, 2) investigate horizontal mass convergence as

a more appropriate diagnostic in an ingredients-based methodology (e.g., McNulty 1978a; Doswell 1987; Johns and Doswell 1992) for forecasting CI, and 3) raise awareness of elevated convection. In section 2 of this article, we review the physical expression of MFC. Section 3 provides a historical account of forecast applications involving MFC, and traces the evolution of MFC into the arena of short-range CI prediction. In section 4, a scale analysis demonstrates the similarity between surface MFC and horizontal mass convergence. In section 5, conceptual models of how MFC or horizontal mass convergence can be applied to CI are constructed and are used as a pretext for discussing an elevated (i.e., convective updrafts not rooted in the local boundary layer) severe thunderstorm case study in section 6. Finally, section 7 provides a summary and concluding discussion.

2. Physical expression

The expression for MFC can be derived from the conservation of water vapor in pressure (p) coordinates:

$$\frac{dq}{dt} = S\,, \tag{1}$$

where

$$\frac{d}{dt} = \frac{\partial}{\partial t} + u\frac{\partial}{\partial x} + v\frac{\partial}{\partial y} + \omega\frac{\partial}{\partial p}\,,$$

u, v, and ω represent the standard three-dimensional wind components in pressure coordinates, and q is the specific humidity. S represents the storage of water vapor, which is the difference between the sources and sinks of water vapor following air parcel motion. S typically takes the form E–C, where E (C) is the evaporation (condensation) rate into the air parcel. Studies employing (1) often assume that all the condensed water immediately precipitates out (P), so that

$S=E-P$ (e.g., Palmén and Holopainen 1962). Further, the mass continuity equation, $\partial u/\partial x + \partial v/\partial y + \partial \omega/\partial p = 0$, allows (1) to be expanded and rewritten in flux form by effectively adding zero to both sides of (1):

$$\frac{\partial q}{\partial t} + u\frac{\partial q}{\partial x} + v\frac{\partial q}{\partial y} + \omega\frac{\partial q}{\partial p} + q\left(\frac{\partial u}{\partial x} + \frac{\partial v}{\partial y} + \frac{\partial \omega}{\partial p}\right) = E - P\,. \tag{2}$$

$$\frac{\partial q}{\partial t} + \frac{\partial}{\partial x}(qu) + \frac{\partial}{\partial y}(qv) + \frac{\partial}{\partial p}(q\omega) = E - P\,.$$

$$\underbrace{\frac{\partial q}{\partial t}}_{\substack{\text{local rate of}\\ \text{change of } q}} + \underbrace{\nabla\cdot(q\mathbf{V}_h)}_{-\text{ horizontal MFC}} + \underbrace{\frac{\partial}{\partial p}(q\omega)}_{-\text{ vertical MFC}} = \underbrace{E-P}_{\substack{\text{sources}\\ \text{andsinks}}}\,, \tag{3}$$

where $\nabla = \hat{\mathbf{i}}\frac{\partial}{\partial x} + \hat{\mathbf{j}}\frac{\partial}{\partial y}$ and $\mathbf{V}_h = (u,v)$. Specifically, (3) expresses the moisture budget for an air parcel, where the terms consist of the local rate of change of q, horizontal moisture flux divergence (the negative of horizontal MFC), the vertical moisture flux divergence (the negative of vertical MFC), and source and sink terms of moisture (specifically, evaporation and precipitation rates).

By vector identity, horizontal MFC[1] (often referred to simply as *moisture convergence* within the forecasting community) can be written as:

$$\text{MFC} = -\nabla\cdot(q\mathbf{V}_h) = -\mathbf{V}_h\cdot\nabla q - q\nabla\cdot\mathbf{V}_h\,, \tag{4}$$

$$\text{MFC} = \underbrace{-u\frac{\partial q}{\partial x} - v\frac{\partial q}{\partial y}}_{\substack{\text{advection}\\ \text{term}}} \underbrace{-q\left(\frac{\partial u}{\partial x} + \frac{\partial v}{\partial y}\right)}_{\substack{\text{convergence}\\ \text{term}}}\,. \tag{5}$$

[1] Although mathematical terminology would refer to (4) as the negative of moisture flux divergence, in this paper, we follow common operational practice and refer to (4) as the moisture flux convergence.

In (5), the *advection term* represents the horizontal advection of specific humidity, whereas the *convergence term* denotes the product of the specific humidity and horizontal mass convergence. This terminology is used throughout the remainder of the paper.

This expression for MFC illustrates that horizontal MFC is only one term in the local tendency of water vapor. Thus, MFC is not capable of acting as a suitable diagnostic for situations where vertical MFC and sources/sinks are occurring. Observations of surface *moisture pooling* (Johns 1993; Glickman 2000) demonstrate the importance of horizontal variations in vertical moisture fluxes (e.g., from vegetation) and boundary-layer mixing height in determining short-term changes in near-surface moisture, and may be a more important factor than advective processes in certain situations.

3. Forecast utility

The application of MFC in weather prediction has focused on three general topics: 1) calculation of large-scale precipitation fields within extratropical cyclones during the 1950s through mid 1960s, 2) as an integral component in the Kuo convective parameterization scheme developed in the 1960s, and, 3) severe local storm prediction as a direct result of 2) (e.g., Hudson 1970, 1971). A more detailed treatment of the history of each of these areas is included in the following subsections. A chronology of observational studies related to these topics is summarized in Table 1.

a. Calculations of precipitation in midlatitude cyclones

Equation (3) can be solved for $P–E$, divided by the acceleration due to gravity g, and vertically integrated over the depth of the atmosphere from the surface $p=p_s$ to $p=0$ (Väisänen 1961; Palmén and Holopainen 1962), yielding

$$\overline{P} - \overline{E} = -\frac{1}{g}\int_0^{p_s} \frac{\partial q}{\partial t} dp - \frac{1}{g}\int_0^{p_s} \mathbf{V}_h \cdot \nabla q dp - \frac{1}{g}\int_0^{p_s} q \nabla \cdot \mathbf{V}_h dp \ , \qquad (6)$$

where the overbar represents a vertical integrated quantity. If one assumes that evaporation $\overline{E}$ is small in areas of intense precipitation and saturation, and that local changes in water vapor content are primarily those owing to advection in synoptic-scale systems (such that the first two terms on the right-hand side are in balance, see references above), then

$$\overline{P} \approx -\frac{1}{g}\int_0^{p_s} q \nabla \cdot \mathbf{V}_h dp \ . \qquad (7)$$

Thus, the precipitation amount is proportional to the vertically integrated product of specific humidity and horizontal mass convergence through the depth of the atmosphere.

The earliest synoptic application of (7) was from moisture budgets to estimate the large-scale precipitation in midlatitude cyclones using rawinsonde observations (Spar 1953; Bradbury 1957; Väisänen 1961; Palmén and Holopainen 1962; Fankhauser 1965). However, advances in numerical weather prediction almost certainly resulted in the phasing out of these attempts beginning in the 1960s, although the concept was theoretically sound (but also quite laborious). The case studies referenced above showed that precipitation calculated from (7) reproduced well the observed spatial pattern of precipitation and the maximum precipitation amount associated with midlatitude cyclones over the United States and the United Kingdom. For instance, Fankhauser (1965) found that the area and time average of vertically integrated MFC over the domain of a warm-sector squall line accounted for 80% of observed rainfall over the region. With the addition of vertically integrated local changes of water vapor with time [first term on the left-hand side of (3)], 95% of the observed rainfall could be accounted for. Limitations to the approach included the inability to sample small-scale horizontal mass convergence with the

rawinsonde network, and the suspension time of cloud droplets prior to being released from the cloud as precipitation, which could be as long as 12–18 h (Bradbury 1957).

b. The Kuo scheme

Kuo (1965, 1974) wished to quantify the latent heat release during condensation in tropical cumulonimbus, the main source of energy in tropical cyclones. He surmised that quantification of the water vapor budget might reveal the magnitude of the vertical motion and latent heat release indirectly. He derived the vertically integrated condensation minus evaporation $\overline{C}-\overline{E}$ as

$$\overline{C}-\overline{E}=(1-b)gM_t, \tag{8}$$

where b represents the storage of moisture and M_t is termed the *moisture accession*:

$$M_t=-\frac{1}{g}\left[\int_0^{p_s}\nabla\cdot(q\mathbf{V}_h)dp+F_{qs}\right]. \tag{9}$$

Moisture accession is the sum of a vertically integrated MFC and F_{qs}, the vertical molecular flux of water vapor from the surface. Kuo (1965) assumed that all the moisture accession goes into making clouds (i.e., b=0), a good assumption where tropical cumulus form in regions of deep conditional instability and large-scale surface horizontal mass convergence. Kuo (1974) found that b was much smaller than 1 in most situations and could be neglected in (8), leading to a direct relationship between the moisture accession and the condensation. Consequently, he argued that cumulus convection in the Tropics would be driven by the large-scale vertically integrated MFC. The use of M_t as a method to parameterize convective clouds is thus termed *the Kuo scheme*.

There are important limitations with the Kuo scheme, however. First, the Kuo scheme was developed initially for tropical cyclone simulations, where the important question is *how*

much latent heat will be released, not *will* latent heat be released. In contrast, the latter is often of central concern to convective forecasters in midlatitudes, particularly in thermodynamic environments possessing an elevated mixed-layer (e.g., Carlson et al. 1983) and some degree of CIN through most (if not all) of the diurnal cycle. More formally, the Kuo formulation assumes convection processes moisture at the rate supplied by the environment [i.e., statistical equilibrium exists, Type I convection (Emanuel 1994, p. 281)]. Conversely, the sudden release of a finite, and typically large, amount of CAPE that has been built up over time is a binary episode [i.e., "triggered" or Type II convection (Emanuel 1994, p. 281)] in which the timing, and even the occurrence of the convection itself, remains a difficult and important forecast problem. Raymond and Emanuel (1993) argue that the assumption of statistical equilibrium is a flaw in the Kuo scheme, because convection is caused by more than just the supply of moisture on the large scale. The binary nature of CI is problematic for both human forecasters and numerical simulations, as was alluded to in the introduction. These issues with the Kuo scheme help explain why well-defined maxima of MFC or horizontal mass convergence may exist in a favorable environment for CI, but CI does not occur because of the presence of capping inversions. Second, these problems with the Kuo scheme are manifested by lower forecast skill scores compared to other convective parameterization schemes in mesoscale numerical models (e.g., Reed et al. 1993; Wang and Seaman 1997). Thus, these criticisms suggest the Kuo scheme may not be an optimal technique for parameterizing cumulus convection in midlatitudes, consequently providing a cautionary pretext for applying MFC to CI.

c. Application of MFC to midlatitude convection

The emergence of the Kuo scheme for tropical convection prompted testing MFC as a measure of the potential for midlatitude convection, particularly storms occurring in

preconvective environments with high CAPE or strong vertical wind shear. Hudson (1970, 1971) was the first to compute vertically integrated MFC and to compare it to the amount of moisture required for cloud development in the midlatitudes for nine severe-weather events, interpreting the ratio between these two quantities as the fraction of convective cloud cover. He computed vertically integrated MFC over a depth from the surface to 10 000 ft (3048 m) MSL because "most of the water vapor is in this layer and because loss of wind data becomes significant above this level" (Hudson 1971, p. 759). Similarly, Kuo (1974) employed the top of his integration at 400 mb because of the perceived poor quality of the upper-air data above this level. Newman (1971), however, argued for using surface hourly observations to compute MFC because of their higher temporal and spatial resolution. As a result, he became the first to calculate surface MFC. The majority of studies since that time have computed surface, not vertically integrated, MFC, to take advantage of the better resolution (Table 1). In section 5, we consider situations in which surface conditions may not be representative of data through a deeper layer, as well as elevated CI, both of which limit the value of surface MFC in those specific scenarios.

Hudson (1970, 1971) and Newman (1971) found the best association between maxima of MFC and convective storms occurred 3 h *after* the time of the MFC analysis. This lag time suggested that surface MFC could be used as a short-range predictive parameter, and this has been noted in other MFC case studies (e.g., Doswell 1977; Negri and Vonder Haar 1980; Waldstreicher 1989). These investigations opened the door for using MFC in real-time severe-weather forecast operations. In the early 1970s, implementation of surface MFC at the National Severe Storms Forecast Center (NSSFC, now the SPC) started with a computer program providing hourly printouts of gridded surface MFC plots 30 minutes after the hour (i.e., "data

time"), which were then hand analyzed by duty forecasters[2] (Ostby 1975). Today, real-time hourly analyses of MFC and other severe weather parameters can be found from a wide variety of Internet sources, including the SPC mesoscale analysis page (http://www.spc.noaa.gov/exper/mesoanalysis/).

In a different effort, surface MFC and its time tendency were included in screening regression procedures (Charba 1975) for the development of an objective severe weather forecast method devised by the Techniques Development Laboratory (TDL) and transmitted to NSSFC and local NWS offices beginning in May 1972. Interestingly, surface MFC was typically the top predictor selected in 1974 and 1975 versions of the regression equations that forecasted severe-storm report location (Charba 1975).

Numerical weather prediction models began to be employed to predict CI in the mid 1970s. McNulty (1978b) found the boundary-layer MFC in the Limited-Area Fine-Mesh Model (LFM) noisy, although many maxima persisted from one 6-h period to another and were associated with severe weather. Charba (1979) produced multiple linear regression equations of surface data and upper-air forecasts from the LFM. Further studies with the Nested-Grid Model (NGM) low-level MFC (derived from the lowest four model levels, approximately the lowest 180 mb) by Nierow (1989), Beckman (1990, 1993), and Fuhs (1996) also suggested the utility of this parameter for forecasting convective storms.

4. Scale analysis

[2] H. Hudson's move from NSSL in Norman, OK to the NSSFC in Kansas City, MO in 1971 likely aided in the implementation of MFC into NSSFC's operational analysis routine.

Recall from (5) that MFC can be written as the sum of two terms: the advection and convergence terms. In this section we deduce the behavior of these terms under synoptic and mesoscale conditions typically found with initiating deep moist convection.

a. Physical considerations

We note that in midlatitude convective situations, q generally falls between 5 and 30 g kg^{-1}; that is, q does not vary by more than one order of magnitude. On the other hand, horizontal divergence at the surface is highly scale dependent (Petterssen 1956, p. 292), varying from 10^{-6} s^{-1} for synoptic- and planetary-scale flows to 10^{-3} s^{-1} near initiating surface-based thunderstorms based on data from research analysis networks (Ulanski and Garstang 1978a; Wilson et al. 1992) and radar (Wilson and Shreiber 1986). For synoptic-scale features with a time scale O(1 day) and a space scale O(1000 km), $|\mathbf{V}_h|$=O(10 m s^{-1}), q=O(10 g kg^{-1}), ∇q= O[1 g kg^{-1} (100 km) $^{-1}$], and $|\nabla \cdot \mathbf{V}_h|$=O($10^{-6}$ s^{-1}). Thus, the advection term $|\mathbf{V}_h \cdot \nabla q|$ of the horizontal MFC equation is O(10^{-4} g kg^{-1} s^{-1}) and the convergence term $|q\nabla \cdot \mathbf{V}_h|$ is an order of magnitude smaller at O(10^{-5} g kg^{-1} s^{-1}). That the advection term dominates the convergence term is consistent with Rasmusson (1967), who found that advection of moisture is the dominant term in controlling the local change of moisture on the largest scales, including monthly and seasonal moisture budgets. The importance of Gulf of Mexico return flow northward across the Great Plains, in advance of spring upper troughs emerging from the southwestern U.S., is one well-known example that emphasizes the importance of moisture advection on synoptic time scales prior to convective events.

On the scale of fronts, however, $|\nabla \cdot \mathbf{V}_h|$ is an order of magnitude larger, O(10^{-5} s^{-1}), such that both the advection and convergence terms are comparable at O(10^{-4} g $kg^{-1}s^{-1}$). For smaller mesoscale boundaries (e.g., lake/sea breezes, active or remnant convective outflow boundaries),

or strong fronts, horizontal mass convergence $|\nabla \cdot \mathbf{V}_h|$ would be at least an order of magnitude larger, O(10^{-4} s^{-1}), implying dominance of the convergence term O(10^{-3} g kg^{-1} s^{-1}).

In a special observational network over south Florida (horizontal resolution of 2.5 km x 2.5 km and time resolution of 5 min), the magnitude of $|\nabla \cdot \mathbf{V}_h|$ was measured as high as 2.7×10^{-3} s^{-1} near developing convective updrafts (Ulanski and Garstang 1978a). Observations of surface MFC of O(10^{-3} g $kg^{-1}s^{-1}$) are well documented in the vicinity of CI in severe-storm case studies (Ostby 1975; Negri and Vonder Harr 1980; Koch and McCarthy 1982). However, most standard wind observing networks are unable to resolve storm-scale MFC, which is likely O(10^{-2} g kg^{-1} s^{-1}) near robust updrafts. Thus, the scale on which MFC and horizontal mass convergence is measured is typically *not* the scale on which convective initiation occurs, a considerable dilemma for researching and forecasting convective initiation (a point beyond the scope of this paper).

The choices for the scalings above are not rigid, but depend on the synoptic situation. For example, very fine-scale measurements along drylines (e.g., Ziegler and Rasmussen 1998) indicate ∇q = O(1 g kg^{-1} km^{-1}), two orders of magnitude larger than that assumed above. Thus, the advection and convergence terms along a dryline could be of comparable magnitude, and might be most important when both terms contribute to positive surface MFC in the case of a retreating (westward-moving) dryline, although this synoptic situation is generally not favorable for CI. CI near drylines has been the subject of extensive study and debate over the years, and may be associated with processes other than near-surface horizontal mass convergence along the dryline boundary (e.g., Ziegler and Rasmussen 1998).

From a forecasting perspective, the spatial distribution of surface observations near mesoscale boundaries and choices in objective analysis procedures can strongly influence the character of the MFC (or horizontal mass convergence) field (e.g., Doswell 1977). Such

nonmeteorological issues can result in a poor surface objective analysis, a problem improved by remote-sensing tools such as radar and visible satellite imagery to better detect boundaries and low-level horizontal mass convergence in real time (e.g., Wilson and Mueller 1993; Wilson et al. 1998). Other objective analysis procedures, such as the so-called "triangle method" (Bellamy 1949), have shown improved performance in the calculation of derivative fields over finite differencing schemes, especially for marginally sampled phenomena and in spatially uneven data distributions (e.g., Doswell and Caracena 1988; Spencer and Doswell 2001). Employing superior objective schemes in operational forecasting environments would likely increase the accuracy of analyzed surface kinematic fields used by forecasters in applications such as CI.

b. Case example

To compare directly the relative magnitude and spatial patterns of the convergence and advection terms with both surface MFC and horizontal mass convergence, surface data for 1800 UTC 4 May 2003 were objectively analyzed at 40-km horizontal grid spacing (Fig. 1). This analysis is the operational objective-analysis routine employed by the SPC (Bothwell et al. 2002), which uses hourly Rapid Update Cycle (RUC) forecasts (Benjamin et al. 2004a,b) as the first-guess field.

At 1800 UTC 4 May 2003, a 990-mb low was centered near the northern Kansas and southern Nebraska border, with a warm front extending east-southeastward into western Missouri and a cold front extending west-southwestward along the surface wind shift in western Kansas and eastern Colorado (Fig. 1). A dryline, extending southward from the low, was moving rapidly eastward across central Kansas, central Oklahoma, and north-central Texas, with a narrow surface moist axis ($q \sim 16$ g kg^{-1}) between the dryline and warm front. An attendant strong 500-mb short-wave trough was moving eastward from Colorado and New Mexico into the

central plains states at this time (not shown). The upper-level forcing combined with instability and low-level moisture resulted in the development of isolated supercells beginning around 1815 UTC near the warm front in northeastern Kansas. Initiation of additional supercellular storms then occurred at 1900–2100 UTC, south of the warm front along the axis of maximum horizontal mass convergence from southeastern Kansas into north-central Texas, just east of the dryline.

Negative moisture advection (–2 to -6×10^{-4} g kg^{-1} s^{-1}) was observed west of the progressive (eastward-moving) dryline, but positive areas of moisture advection of the same magnitude occurred in only very small areas near the warm front in eastern Kansas and along the cold front in west-central Kansas (Fig. 1a). The convergence term (Fig. 1b) was most coherent near the surface low, along the warm front, and along the cold front in western Kansas and eastern Colorado. The convergence term was also large along the dryline (Fig. 1b). The convergence term was relatively effective in highlighting the boundaries of interest, with small-scale features (or noise from the RUC first guess) dominating elsewhere across the analysis domain. The surface MFC largely reflected the convergence term, with the exception of the strong negative area west of the dryline (cf. Figs. 1c and 1b).

The scaling arguments suggest that surface MFC can serve as an effective tool to detect mesoscale boundaries. However, surface horizontal mass convergence can serve the same purpose because it largely determines the surface MFC field (cf. Figs. 1c and 1d). Forecasters may wish to compare MFC with horizontal mass convergence in convective situations to see these similarities.

5. Conceptualized variations of convective initiation

The necessary ingredients for deep moist convection (moisture, instability, and lift) (e.g., McNulty 1978a; Doswell 1987; Johns and Doswell 1992) provide a framework for further discussion. Although surface MFC *relates* to each of the necessary ingredients in some way, problems can arise when surface MFC is employed as a *proxy* for the ingredients. Because the spatial distribution of MFC closely matches that of horizontal mass convergence, we show how horizontal mass convergence relates to the CI process and location in this section. A generalized discussion and a brief example of elevated thunderstorm development follow.

Updrafts leading to deep moist convection are necessarily associated with subcloud horizontal mass convergence owing to the constraints of mass continuity. This relationship, however, is only a diagnostic relationship that applies instantaneously. Thus, no prognostic information is included. Sustained low-level horizontal mass convergence over time may eventually result in the cap being compromised and the initiation of deep, moist convection, thus providing some forecast utility. Unfortunately, the uncertainties in the magnitude of ascent, the locations of ascent, and the four-dimensional structure of the cap is what makes convective forecasting such a challenge. One nonmeteorological issue that affects our ability to diagnose these features is that the scale of horizontal mass convergence associated with developing convection may not be well sampled by standard observational data networks (section 4a). Other issues are meteorological, and are shown in schematic diagrams in Fig. 2.

In Fig. 2a, surface horizontal mass convergence is part of a deep tropospheric circulation as might be observed along a front with associated strong synoptic- or mesoscale forcing. These systems are efficient in eliminating convective inhibition through strong midlevel ascent, and the presence of moisture and instability often results in the surface horizontal mass convergence (or

MFC maxima) being closely representative of the initiation location. Many published MFC case studies (Table 1) involve initiation of this type.

In Fig. 2b, the surface horizontal mass convergence is part of a shallow vertical circulation confined to the PBL, above which there is usually a spatially and temporally varying degree of CIN. In the absence of large-scale forcing for ascent, or in the presence of midlevel subsidence (e.g., Stensrud and Maddox 1988), convective development may be precluded. Even when CIN is small (in absolute value), incipient updrafts may weaken because of entrainment of low relative humidity air into the updraft, particularly when forcing for ascent is weak. These factors are difficult to quantify in an operational setting and contribute in large measure to the uncertainty in short-range convective forecasts.

In Fig. 2c, the surface horizontal mass convergence is representative of a vertical circulation with considerable slope. Such situations include, not only warm fronts, but subtle differences in boundary-layer characteristics and depth arising from remnant outflow boundaries, differential cloud cover, or varying land surface characteristics. In these situations, localized regions of warm advection can result in sufficient lift for convective development. Furthermore, convective development may be horizontally displaced from the surface horizontal mass convergence maxima and rooted above the local boundary layer (and above a relatively cool air mass). Indeed, one of the anonymous reviewers noted that some forecasters look at horizontal mass convergence at levels above the surface, in search of areas where CI may occur. Such scenarios may help explain the observed displacement of storms downstream of the surface MFC maxima (e.g., Hirt 1982). Severe hail and locally heavy rainfall are the most common threats from such elevated storms, with the potential for tornadoes and damaging winds reduced owing to the stable near-surface stratification. The relative strength of surface-based CIN and the

elevated storm updrafts modulate the ability of the individual storms to become surface-based at some point after initiation. Elevated thunderstorms have been discussed by Colman (1990a,b) and Moore et al. (1998, 2003). We believe the forecast community could benefit from additional research in this area because the timing and location of elevated severe thunderstorm episodes are difficult to predict.

Another example of elevated convection appears in Fig. 2d. Here, subcloud horizontal mass convergence occurs above the PBL, such that an association between the surface horizontal mass convergence/MFC and CI does not exist (e.g., Schaefer and Doswell 1980). Unlike Fig. 2c in which PBL air is displaced but still processed as the main source of potential instability in a relatively undiluted fashion, Fig. 2d depicts a vertical circulation without direct connection to PBL for its source of potential instability. This situation is illustrated further using an example from 27 May 2004 in section 6.

These four conceptual models in Fig. 2 illustrate the variety of different relationships between horizontal mass convergence and convective development. Clearly, a one-size-fits-all relationship between horizontal mass convergence (or MFC) and CI is not possible.

6. A case of elevated severe thunderstorms

The surface objective analysis at 1500 UTC on 27 May 2004 shows a weak surface cyclone over southeastern Kansas, with a surface boundary and associated region of maximum surface horizontal convergence extending from northeastern Kansas eastward across northern sections of Missouri (Fig. 3d). This boundary was developed in part through outflow from early morning thunderstorms across eastern Kansas and central Missouri. Surface winds were generally southerly equatorward of the boundary, but became weak and ill-defined near and north of the zone of maximum surface horizontal mass convergence. Surface specific humidity

values were about 12–13 g kg^{-1} over northern Missouri and southern Iowa. Consistent with the previous example in Fig. 1, the convergence term dominates the surface MFC (cf. Figs. 3b and 3c) because the advection term is relatively weak (Fig. 3a). Likewise, the similarity of surface MFC to surface horizontal mass convergence is quite striking (cf. Figs. 3c and 3d); surface MFC provides no tangible advantage to the forecaster over surface horizontal mass convergence in this case.

Visible satellite imagery reveals that the initial convective development occurred in southwest Iowa around 1515 UTC, displaced about 130 km north of the surface MFC maxima (Fig. 4) and collocated surface boundary and surface horizontal mass convergence maxima (Fig. 3d). The near-surface stable layer in 1200 UTC soundings at Topeka, Kansas, (Fig. 5a) and Omaha, Nebraska, (Fig. 5b) is likely inhibiting CI in the region of the surface boundary. An essential feature of the Topeka sounding pertinent to this case is the saturated layer at 820–780 mb (Fig. 5a). Parcels within this layer are potentially buoyant (CAPE ~ 1500 J kg^{-1}), though capped above by the elevated mixed layer air around 700 mb. Additionally, the 780–530-mb layer is much warmer at Topeka than Omaha (cf. Figs 5a,b), with the temperature difference maximized near 700 mb (10°C at Topeka vs 4°C at Omaha). This strong gradient in midlevel temperature was located along and south of the upper-level cloud band evident in visible imagery from south-central Nebraska into central Iowa, which was associated with a compact short-wave trough across central Nebraska (not shown), likely aiding in synoptic-scale forcing for ascent.

A sounding from the RUC initialized at 1500 UTC in southern Iowa near the time of convective initiation is shown in Fig. 5c (location of sounding shown by "X" in Fig. 6). The sounding was modified slightly for 1500 UTC surface conditions near the developing storms using a temperature of 70°F (21.1°C) and a dewpoint of 62°F (16.7°C), yielding a surface-based

convective inhibition of –80 J kg^{-1} (Fig. 5c). The RUC sounding does not resolve fully the moist layer between 800–750 mb. However, animations of visible satellite imagery indicate a distinct northward surge of moisture and a band of thicker stratus clouds (moving northward at around 10 m s^{-1}) into southwestern Iowa just prior to initiation, invigorating existing weaker convective updrafts in the region. Additionally, the 1455 UTC and 1515 UTC surface observations at Clarinda, Iowa (ICL), in east-central Page County (see Fig. 6 for the location), indicated broken clouds at 4900 ft (1493 m) AGL. These observations were within 25 km of, and nearly coincident in time and space with, the initial development of deep moist convection. This cloud height corresponds well with the base height of the moist layer observed at Topeka at 1200 UTC. If the RUC sounding from southwest Iowa (Fig. 5c) is modified by the moist layer from the observed Topeka sounding (Fig. 5a), the sounding that results (Fig. 5d) yields a CAPE of 2100 J kg^{-1} without CIN for a parcel lifted from 820 mb. Combined with ascent provided by the approaching short-wave trough, this moist layer contributed to initiation of elevated supercells in prevailing strong westerly shear (the shear magnitude from the base of the moist layer up 6 km was 22.5 m s^{-1}). The convection was quick to produce numerous reports of large hail and isolated damaging winds through 1900 UTC (Fig. 6). As the day progressed, diurnal heating reduced surface-based CIN and ultimately allowed thunderstorm updrafts to become rooted in the boundary layer and continued producing severe weather as they tracked southeastward across the northern half of Missouri with up to 4-in (10.2-cm) diameter hail and isolated tornadoes (not shown).

7. Final thoughts

The forecaster's primary intent in the subjective use of surface MFC is to infer locations of developing vertical circulations that might aid in the release of potential instability, allowing for CI. Successful use of surface MFC is limited to those occasions when upward vertical motion associated with incipient CI can be inferred through a depiction of the associated surface horizontal mass convergence and subjective application of the continuity equation. As such, the importance of boundaries as a focus for CI cannot be understated. However, we show that horizontal mass convergence of the magnitude found along mesoscale boundaries implies dominance of the convergence term in the expression for MFC because the modulating influence of q and moisture advection is comparatively small. This argument suggests that horizontal mass convergence will identify surface boundaries equally as well as surface MFC, if not better, and has a more rigorous link to the ingredients-based methodology for deep moist convection.

The utility of surface horizontal mass convergence for forecasting CI has been studied for numerous years, with the earliest references extending back to the Thunderstorm Project (e.g., Byers and Braham 1949, p. 53). Subsequent research also has shown a relationship between surface horizontal mass convergence and convective storms (e.g., Breiland 1958; Matsumoto et al. 1967; Anderson and Uccellini 1973; Ulanski and Garstang 1978a,b; Peslen 1980). More recently, Wilson and collaborators have quantified the importance of surface horizontal mass convergence to storms through real-time forecasting experiments and field projects (e.g., Wilson and Schreiber 1986; Wilson and Mueller 1993; Wilson and Megenhardt 1997; Wilson et al. 1988, 1998, 2004). Thus, the connection between horizontal mass convergence and CI (as part of an ingredients-based forecasting methodology) is well posed theoretically and empirically justifiable.

We expect that forecasters who have used MFC for years may be reluctant to change, claiming it has worked well for them in past forecasting situations. To support or refute such claims, a comprehensive climatology of MFC maxima and convective-storm initiation locations would need to be constructed. Indeed, no such climatology showing the effectiveness or ineffectiveness of MFC has been performed. In considering the construction of such a climatology, decisions would have to be made about the minimum magnitude to be considered a MFC maximum, how long a MFC maximum must exist to be considered related to convective initiation, the distance criteria to be adopted for proximity to the convective storm initiation, etc. Such issues have been discussed qualitatively (e.g., Newman 1971; Charba 1979; Hirt 1982; Beckman 1990, 1993; Fuhs 1996), but a rigorous climatology would need to quantify these numbers. Moreover, generating a climatology of horizontal mass convergence would raise the same questions. Instead, a more constructive research effort should be focused on the physical processes that lead to convective initiation. Such efforts should emphasize the advantages of an ingredients-based methodology, in which forcing for ascent (and its related field of horizontal mass convergence) serves as an indirect measure of lift.

Although scientifically more appropriate, application of horizontal mass convergence for predicting CI suffers from many of the same problems as MFC. First, a potentially unstable boundary layer air mass may be capped, and therefore the vertical circulation inferred from surface horizontal mass convergence is likely insufficient to carry air parcels to their LFC (e.g., Fig. 2b). Second, midlevel entrainment may curtail convective growth despite otherwise favorable conditions. Third, available surface data may be inadequate to resolve the scale of surface horizontal mass convergence associated with the upward vertical motion. Fourth, the ascending branch of motion may contain considerable slope, allowing for development of deep

moist convection downstream of surface MFC or horizontal mass convergence maxima. Fifth, the lower branch of a vertical circulation associated with deep moist convection may not occur at the surface, but aloft. Finally, such situations curtail the more general applicability of surface diagnostics, either MFC or horizontal mass convergence, because the near-surface conditions may not be representative of convectively processed air.

While these problems are not easily alleviated, alternatives to traditional techniques such as surface MFC are needed. There is still a role for intelligently designed, scientifically sound, empirically based studies in this regard. Nevertheless, a thorough physical understanding of MFC or any other diagnostic is essential for real-time forecasting, particularly for assessing its limitations and quickly recognizing situations where alternative approaches should be taken.

Lastly, a sidelight of this paper is the importance of elevated convection. The version of the Eta model with the Kain–Fritsch cumulus parameterization (Kain et al. 2003b) provides as one of its outputs the pressure of the updraft source air (Kain et al. 2003a). Operational experience at the SPC with this field suggests that as many as 50% of convective storms have updraft source levels above the surface (J. Kain 2003, personal communication). This observation is supported by the nearly even split between surface-based and elevated CI episodes during IHOP (Wilson and Roberts 2004). Elevated CI underscores the importance of determining the source of moist and unstable air for convective development, which is generally not trivial given the more sparse distribution of direct observations aloft. Although the frequency of correct forecasts can be increased through synthesis of available data resources in three dimensions, more work from the research community, aimed at new predictive strategies for elevated CI, would be beneficial to forecasters.

Continued research on all aspects of the CI process, including the importance of surface fluxes, should lead to the emergence of new physically based parameters, conceptual models, and improved numerical models incorporating small-scale processes. Coupled with new observational data sources, increased accuracy in CI forecasts should continue to be realized in the years ahead.

Acknowledgments. We wish to thank the following individuals for their discussions pertaining to this project: Phillip Bothwell (SPC), Chuck Doswell (OU/CIMMS), Bob Johns (retired), Jack Kain (NSSL), Jim Moore (St. Louis Univ.), Steve Sherwood (Yale Univ.), and Steve Weiss (SPC). We also acknowledge the three anonymous reviewers, whose comments helped us clarify and improve the manuscript. Funding for Schultz was provided by NOAA/OAR/NSSL under NOAA–OU Cooperative Agreement NA17RJ1227.

REFERENCES

Anderson, C. E., and L. W. Uccellini, 1973: Studies of meteorological factors involved in the formation of severe local storms in the northeast Colorado region. Preprints, *Eighth Conf. on Severe Local Storms,* Denver, CO, Amer. Meteor. Soc., 84–89.

Beckman, S. K., 1990: A study of 12-h NGM low-level moisture flux convergence centers and the location of severe thunderstorms/heavy rain. Preprints, *16th Conf. on Severe Local Storms*, Kananaskis Park, Alberta, Canada, Amer. Meteor. Soc., 78–83.

_____, 1993: Preliminary results of a study on NGM low-level moisture flux convergence and the location of severe thunderstorms. Preprints, *17th Conf. on Severe Local Storms,* St. Louis, MO, Amer. Meteor. Soc., 138–142.

Bellamy, J. C., 1949: Objective calculations of divergence, vertical velocity, and vorticity. *Bull. Amer. Meteor. Soc.*, **30**, 45–49.

Benjamin, S. G., G. A. Grell, J. M. Brown, T. G. Smirnova, and R. Bleck, 2004a: Mesoscale weather prediction with the RUC hybrid isentropic–terrain-following coordinate model. *Mon. Wea. Rev.,* **132**, 473–494.

_____, D. Dévényi, S. S. Weygandt, K. J. Brundage, J. M. Brown, G. A. Grell, D. Kim, B. E. Schwartz, T. G. Smirnova, T. L. Smith, and G. S. Manikin, 2004b: An hourly assimilation–forecast cycle: The RUC. *Mon. Wea. Rev.,* **132**, 495–518.

Bothwell, P. D., 1988: Forecasting convection with the AFOS Data Analysis Programs (ADAP-VERSION 2.0). NOAA Technical Memorandum NWS SR-122, 92 pp.

_____, J. A. Hart, and R. L. Thompson, 2002: An integrated three-dimensional objective analysis scheme in use at the Storm Prediction Center. Preprints, *21st Conf. on Severe Local Storms,* San Antonio, TX, Amer. Meteor. Soc., J117–J120.

Bradbury, D. L., 1957: Moisture analysis and water budget in three different types of storms. *J. Meteor.*, **14**, 559–565.

Breiland, J. G., 1958: Meteorological conditions associated with the development of instability lines. *J. Meteor.*, **15**, 297–302.

Byers, H. R., and R. R. Braham, Jr., 1949: *The Thunderstorm.* U.S. Govt. Printing Office, 287 pp.

Carlson, T. N., S. G. Benjamin, G. S. Forbes, and Y.-F. Li, 1983: Elevated mixed layers in the regional severe storm environment: Conceptual model and case studies. *Mon. Wea. Rev.,* **111**, 1453–1473.

Charba, J. P., 1975: Operational scheme for short range forecasts of severe local weather. Preprints, *Ninth Conf. on Severe Local Storms,* Norman, OK, Amer. Meteor. Soc., 51–57.

_____, 1979: Two to six hour severe local storm probabilities: An operational forecasting system. *Mon. Wea. Rev*., **107**, 268–282.

Colman, B. R., 1990a: Thunderstorms above frontal surfaces in environments without positive CAPE. Part I: A climatology. *Mon. Wea. Rev.,* **118,** 1103–1121.

_____, 1990b: Thunderstorms above frontal surfaces in environments without positive CAPE. Part II: Organization and instability mechanisms. *Mon. Wea. Rev.,* **118,** 1123–1144.

Doswell, C. A. III, 1977: Obtaining meteorologically significant surface divergence fields through the filtering property of objective analysis. *Mon. Wea. Rev.*, **105**, 885–892.

_____, 1982: The operational meteorology of convective weather. Volume 1: Operational mesoanalysis. NOAA Technical Memorandum NWS NSSFC-5, 135 pp.

_____, 1987: The distinction between large-scale and mesoscale contribution to severe convection: A case study example. *Wea. Forecasting*, **2**, 3–16.

_____, and F. Caracena, 1988: Derivative estimation from marginally sampled vector point functions. *J. Atmos. Sci.*, **45**, 242–253.

Emanuel, K.A., 1994: *Atmospheric Convection*. Oxford University Press, 580 pp.

Fankhauser, J. C., 1965: A comparison of kinematically computed precipitation with observed convective rainfall. National Severe Storms Laboratory Report 25, Norman, OK, 28 pp.

Fritsch, J. M., and R. E. Carbone, 2004: Improving quantitative precipitation forecasts in the warm season: A USWRP research and development strategy. *Bull. Amer. Meteor. Soc.*, **85**, 955–965.

Fuhs, M. J., Cited 1996: An evaluation of 12 and 18 hour NGM low-level moisture flux convergence and the proximity of severe thunderstorms. NWS Tech. Attachment 96-02. [Available online at http://www.crh.noaa.gov/techa/ta6/tech9602/9602.html.]

Glickman, T. S., Ed., 2000: *Glossary of Meteorology*. 2d ed. Amer. Meteor. Soc., 855 pp.

Hirt, W. D., 1982: Short-term prediction of convective development using dew point convergence. Preprints, *Ninth Conf. on Weather Forecasting & Analysis,* Seattle, WA, Amer. Meteor. Soc., 201–205.

Hudson, H. R., 1970: On the relationship between horizontal moisture convergence and convective cloud formation. ESSA Tech. Memo. ERLTM-NSSL 45, 29 pp.

_____, 1971: On the relationship between horizontal moisture convergence and convective cloud formation. *J. Appl. Meteor.*, **10**, 755–762.

Johns, R. H., 1993: Meteorological conditions associated with bow echo development in convective storms. *Wea. Forecasting*, **8**, 294–299.

_____, and C. A. Doswell III, 1992: Severe local storms forecasting. *Wea. Forecasting,* **7,**

588–612.

Kain, J. S., M. E. Baldwin, and S. J. Weiss, 2003a: Parameterized updraft mass flux as a predictor of convective intensity. *Wea. Forecasting,* **18,** 106–116.

_____, M. E. Baldwin, P. R. Janish, S. J. Weiss, M. P. Kay, and G. W. Carbin, 2003b: Subjective verification of numerical models as a component of a broader interaction between research and operations. *Wea. Forecasting,* **18,** 847–860.

_____, P. R. Janish, S. J. Weiss, M. E. Baldwin, R. S. Schneider, and H. E. Brooks, 2003c: Collaboration between forecasters and research scientists at the NSSL and SPC: The Spring Program. *Bull. Amer. Meteor. Soc.,* **84,** 1797–1806.

Koch, S. E., and J. McCarthy, 1982: The evolution of an Oklahoma dryline. Part II: Boundary-layer forcing of mesoconvective systems. *J. Atmos. Sci.,* **39,** 237–257.

Korotky, W. D., 1990: The Raleigh tornado of November 28, 1988: The evolution of a tornadic environment. Preprints, *16th Conf. on Severe Local Storms,* Kananaskis Park, Alberta, Canada, Amer. Meteor. Soc., 532–537.

Krishnamurti, T. N., 1968: A calculation of percentage area covered by convective clouds from moisture convergence. *J. Appl. Meteor.*, **7**, 184–195.

Kuo, H. L., 1965: On formation and intensification of tropical cyclones through latent heat release by cumulus convection. *J. Atmos. Sci.*, **22**, 40–63.

_____, 1974: Further studies of the parameterization of the influence of cumulus convection on large-scale flow. *J. Atmos. Sci.*, **31**, 1232–1240.

Matsumoto, S., K. Ninomiya, and T. Akiyama, 1967: Cumulus activities in relation to the mesoscale convergence field. *J. Meteor. Soc. Japan,* **45,** 292–305.

McNulty, R. P., 1978a: On upper tropospheric kinematics and severe weather occurrence. *Mon. Wea. Rev.*, **5**, 662–672.

_____, 1978b: On the potential use of LFM II boundary layer moisture and moisture convergence in convective forecasting. Preprints, *Seventh Conf. on Weather Forecasting and Analysis*, Silver Spring, MD, Amer. Meteor. Soc., 88–93.

Moller, A. R., 2001: Severe local storms forecasting. *Severe Convective Storms, Meteor. Monogr.*, No. 50, Amer. Meteor. Soc., 433–480.

Moore, J. T., and J. M. Murray, 1982: The contribution of surface, horizontal moisture convergence to the severe convection of 10–11 April 1979. *Natl. Wea. Dig.*, **7**(1), 15–23.

_____, A. C. Czarnetzki, and P. S. Market, 1998: Heavy precipitation associated with elevated thunderstorms formed in a convectively unstable layer aloft. *Meteor. Appl.*, **5**, 373–384.

_____, F. H. Glass, C. E. Graves, S. M. Rochette, and M. J. Singer, 2003: The environment of warm-season elevated thunderstorms associated with heavy rainfall over the central United States. *Wea. Forecasting,* **18,** 861–878.

Negri, A. J., and T. H. Vonder Haar, 1980: Moisture convergence using satellite-derived wind fields: A severe local storm case study. *Mon. Wea. Rev.*, **108**, 1170–1182.

Newman, W. R., 1971: The relationship between horizontal moisture convergence and severe storm occurrences. M.S. thesis, School of Meteorology, University of Oklahoma, 54 pp. [Available from School of Meteorology, University of Oklahoma, 100 E. Boyd, Rm. 1310, Norman, OK 73019.]

Nierow, A., 1989: An evaluation of the NGM's low-level moisture convergence forecasts

in predicting heavy precipitation/severe weather. Preprints, *12th Conf. on Weather Analysis and Forecasting,* Monterey, CA, Amer. Meteor. Soc., 626–630.

Ostby, F. P. Jr, 1975: An application of severe storm forecast techniques to the outbreak of June 8, 1974. Preprints, *Ninth Conf. on Severe Local Storms,* Norman, OK, Amer. Meteor. Soc., 7–12.

Palmén, E., and E. O. Holopainen, 1962: Divergence, vertical velocity and conversion between potential and kinetic energy in an extratropical disturbance. *Geophysica*, **8**, 89–113.

Peslen, C. A., 1980: Short-interval SMS wind vector determinations for a severe local storms area. *Mon. Wea. Rev.,* **108,** 1407–1418.

Petersen, R. A., W. F. Feltz, J. Schaefer, and R. Schneider, 2000: An analysis of low-level moisture-flux convergence prior to the 3 May 1999 Oklahoma City tornadoes. Preprints, *20th Conf. on Severe Local Storms,* Orlando, FL, Amer. Meteor. Soc., 619–621.

Petterssen, S., 1956: *Weather Analysis and Forecasting. Vol. 1, Motion and Motion Systems*. 2d ed. McGraw-Hill, 428 pp.

Rasmusson, E. M., 1967: Atmospheric water vapor transport and the water balance of North America: Part I. Characteristics of the water vapor flux field. *Mon. Wea. Rev.,* **95,** 403–426.

Raymond, D. J., and K. A. Emanuel, 1993: The Kuo cumulus parameterization. *The Representation of Cumulus Convection in Numerical Models, Meteor. Monogr.*, No. 46, Amer. Meteor. Soc., 145–147.

Reed, R. J., G. A. Grell, and Y.-H. Kuo, 1993: The ERICA IOP 5 storm. Part II:

Sensitivity tests and further diagnosis based on model output. *Mon. Wea. Rev.*, **121**, 1595–1612.

Schaefer, J. T., and C. A. Doswell III, 1980: The theory and practical application of antitriptic balance. *Mon. Wea. Rev.*, **108,** 746–756.

Spar, J., 1953: A suggested technique for quantitative precipitation forecasting. *Mon. Wea. Rev.*, **81**, 217–221.

Spencer, P. L., and C. A. Doswell III, 2001: A quantitative comparison between traditional and line integral methods of derivative estimation. *Mon. Wea. Rev.*, **129**, 2538–2554.

Stensrud, D. J., and R. A. Maddox, 1988: Opposing mesoscale circulations: A case study. *Wea. Forecasting*, **3**, 189–204.

Tegtmeier, S. A., 1974: The role of the surface, sub-synoptic, low pressure system in severe weather forecasting. M.S. thesis, School of Meteorology, University of Oklahoma, 66 pp. [Available from School of Meteorology, University of Oklahoma, 100 E. Boyd, Rm. 1310, Norman, OK 73019.]

Ulanski, S. L., and M. Garstang, 1978a: The role of surface divergence and vorticity in the life cycle of convective rainfall. Part I: Observation and analysis. *J. Atmos. Sci.*, **35**, 1047–1062.

Ulanski, S. L., and M. Garstang, 1978b: The role of surface divergence and vorticity in the life cycle of convective rainfall. Part II: Descriptive model. *J. Atmos. Sci.*, **35**, 1063–1069.

Väisänen, A., 1961: Investigation of the vertical air movement and related phenomena in selected synoptic situations. *Commentationes Physico-Mathematicae, Societas Scientiarum Fennica,* **26**(7), 1–73.

Waldstreicher, J. S., 1989: A guide to utilizing moisture flux convergence as a predictor of convection. *Natl. Wea. Dig.*, **14**(4), 20–35.

Wang, W., and N. L. Seaman, 1997: A comparison study of convective parameterization schemes in a mesoscale model. *Mon. Wea. Rev.*, **125**, 252–278.

Weckwerth, T. M., and Coauthors, 2004: An overview of the International H_2O Project (IHOP_2002) and some preliminary highlights. *Bull. Amer. Meteor. Soc.*, **85**, 253–277.

Wilson, J. W., and W. E. Schreiber, 1986: Initiation of convective storms at radar-observed boundary-layer convergence lines. *Mon. Wea. Rev.,* **114,** 2516–2536.

_____, and C. K. Mueller, 1993: Nowcasts of thunderstorm initiation and evolution. *Wea. Forecasting,* **8,** 113–131.

_____, and D. L. Megenhardt, 1997: Thunderstorm initiation, organization, and lifetime associated with Florida boundary layer convergence lines. *Mon. Wea. Rev.,* **125,** 1507–1525.

_____, and R. D. Roberts, 2004: Thunderstorm initiation and evolution during IHOP: Implications for aviation thunderstorm nowcasting. Preprints, *22nd Conf. on Severe Local Storms*, Hyannis, MA, Amer. Meteor. Soc., CD-ROM, J1.1.

_____, J. A. Moore, G. B. Foote, B. Martner, A. R. Rodi, T. Uttal, and J. M. Wilczak, 1988: Convection Initiation and Downburst Experiment (CINDE). *Bull. Amer. Meteor. Soc.,* **69,** 1328–1348.

_____, G. B. Foote, N. A. Crook, J. C. Fankhauser, C. G. Wade, J. D. Tuttle, C. K. Mueller, and S. K. Krueger, 1992: The role of boundary-layer convergence zones and horizontal rolls in the initiation of thunderstorms: A case study. *Mon. Wea. Rev.*, **120**, 1785–1815.

_____, N. A. Crook, C. K. Mueller, J. Sun, and M. Dixon, 1998: Nowcasting thunderstorms: A status report. *Bull. Amer. Meteor. Soc.*, **79,** 2079–2099.

_____, E. E. Ebert, T. R. Saxen, R. D. Roberts, C. K. Mueller, M. Sleigh, C. E. Pierce, and A. Seed, 2004: Sydney 2000 Forecast Demonstration Project: Convective storm nowcasting. *Wea. Forecasting,* **19,** 131–150.

Ziegler, C. L., and E. N. Rasmussen, 1998: The initiation of moist convection at the dryline: Forecasting issues from a case study perspective. *Wea. Forecasting*, **13**, 1106–1131.

TABLE LIST

FIGURE LIST

Fig. 1 Surface objective analysis valid at 1800 UTC on 4 May 2003. Sea-level pressure (thick solid lines every 2 mb), specific humidity (thin solid lines every 2 g kg^{-1}). Shaded regions represent (a) the advection term in MFC expression (10^{-4} g kg^{-1} s^{-1}), where positive values represent moist advection, (b) the convergence term in MFC expression (10^{-4} g kg^{-1} s^{-1}), where positive values represent convergence, (c) the total moisture flux convergence (10^{-4} g kg^{-1} s^{-1}),where positive values represent positive MFC, and (d) the horizontal mass convergence of the total wind ($10^{-5}s^{-1}$), where negative values represent horizontal mass divergence. Thin dashed lines (thin solid lines) delineate negative (positive) values associated with shaded regions for each panel. Pennant, barb, and half-barb represent wind speeds of 25, 5, and 2.5 m s^{-1}, respectively.

Fig. 2 Schematic of subcloud horizontal mass convergence (conv) as it relates to cumulus convection (represented by cloud outline). Arrows represent streamlines. Thick dashed line indicates top of PBL. (a) Surface horizontal mass convergence maximum is associated with a deep tropospheric circulation and deep moist convection. (b) Surface horizontal mass convergence maximum is associated with shallow cumulus development owing to midlevel subsidence and/or a capping inversion. (c) Surface horizontal mass convergence maximum is located near change in boundary layer depth. Thin dashed line indicates isentropic surfaces. (d) Horizontal mass convergence maximum is rooted above the local boundary layer.

Fig. 3 As in Fig. 1, except for 1500 UTC on 27 May 2004, and specific humidity contour interval is 1 g kg^{-1}.

Fig. 4 *GOES-12* 1-km visible satellite imagery for 27 May 2004: (a) 1515 UTC and (b) 1602 UTC. Surface moisture flux convergence (dotted lines, 10^{-4} g kg^{-1} s^{-1}, negative values only) from SPC surface objective analysis (Bothwell et al. 2002) at (a) 1500 UTC and (b) 1600 UTC.

Fig. 5 Skew *T*–log *p* plots of observed temperature (dark gray lines) and dewpoint temperature (light gray lines) for 1200 UTC 27 May 2004: (a) Topeka, KS, and (b) Omaha, NE. (c) RUC-2 0-h forecast sounding with modified surface conditions valid 1500 UTC 27 May 2004 near the Missouri/Iowa border (see "X" in Fig. 6 for location). (d) As in (c), except sounding is modified using low-level moist layer found on 1200 UTC Topeka sounding in (a). Horizontal bars represent vertical distribution of vertical motion (μb s^{-1}). Pennant, barb, and half-barb represent wind speeds of 25, 5, and 2.5 m s^{-1}, respectively.

Fig. 6 Preliminary National Weather Service storm report data for 1600–1900 UTC 27 May 2004 across northern Missouri and southern Iowa. Location of RUC sounding in Fig. 5c,d is denoted by "X" in southwestern Ringgold County, Iowa. Clarinda, Iowa is denoted by ICL. County borders are indicated by the gray lines with county names listed within.

TABLE 1. Chronology of published studies involving moisture flux convergence for applications of: 1) estimation of large-scale precipitation amounts (P), 2) convective initiation or prediction of severe weather location (CI), 3) percent sky coverage by convective clouds in the Tropics (T), and 4) verification of divergence values used in the kinematic method of calculating vertical motion (D).

Author(s)	Application	Cases	Geographic region(s)	Method of computation over analysis domain	Dominant convective mode	strength of synoptic forcing
Spar (1953)	P	1	lower Miss. Valley to Southeast U.S.	integrated MFC in 50-mb layers, sfc to 400 mb using rawinsondes Qualitative	N/A	strong
Bradbury (1957)	P	3	Central and eastern U.S.	integrated MFC in 100-mb layers, sfc to 400 mb using rawinsondes	N/A	strong
Väisänen (1961)	P, D	1	United Kingdom	integrates divergence term of MFC in 100-mb layers,	N/A	strong

				sfc to 500 mb, using rawinsondes		
Palmén and Holopainen (1962)	P, D	1	Central U.S.	integrated MFC from the sfc to 400mb, using standard isobaric levels and rawinsondes	N/A	strong
Fankhauser (1965)	P	1	Central and southern Plains	integrated MFC and local change of q w.r.t. time in 50-mb layers, sfc to 300 mb from rawinsondes	squall-line	strong
Krishnamurti (1968)	T	1	NW Carribean Sea	Kuo (1965) scheme. Includes MFC integration in 50-mb layers, 900-100mb from aircraft reconnaissance	scattered cellular storms and storm clusters	moderate (easterly wave)

				data		
Hudson (1970)	CI	9	Central and eastern U.S.	integrated MFC (density included) from sfc-10 000 ft using rawinsondes. Integration interval unspecified.	various	strong
Newman (1971)	CI	5	Central and eastern U.S.	MFC at the surface, based on 3-hourly observations	various	strong
Tegtmeier (1974)	CI	4	Southern Plains	MFC at the surface, based on hourly observations	supercells	moderate
Ostby (1975)	CI	1	Southern Plains	MFC at the surface, analyses available to	supercells	strong

				forecasters in real-time		
Doswell (1977)	CI	1	Southern Plains	MFC at the surface, based on hourly observations	supercells	moderate
Schaefer and Doswell (1980)	CI	5	Central and southern U.S.	MFC at the surface and using the antitriptic winds	various	unknown
Negri and Vonder Haar (1980)	CI	1	Southern Plans	MFC using surface q, and satellite-derived boundary layer motions based on cumulus clouds	supercells	moderate
Hirt (1982)	CI	4	Plains	surface dewpoint convergence	various	weak

Koch and McCarthy (1982)	CI	1	Southern Plains	surface equivalent potential temperature flux	supercells	strong
Moore and Murray (1982)	CI	1	Southern Plains	MFC at the surface, based on hourly observations	supercells	strong
Waldstreicher (1989)	CI	1	Northeast U.S.	MFC at the surface, based on hourly observations	bow echo	moderate
Korotky (1990)	CI	1	North Carolina	MFC at the surface, based on hourly observations	supercells	strong
Petersen et al. (2000)	CI	1	Southern Plains	Time-series of MFC in lowest 5000 m based on Wind Profiler Network data and interferometer instruments	supercells	moderate

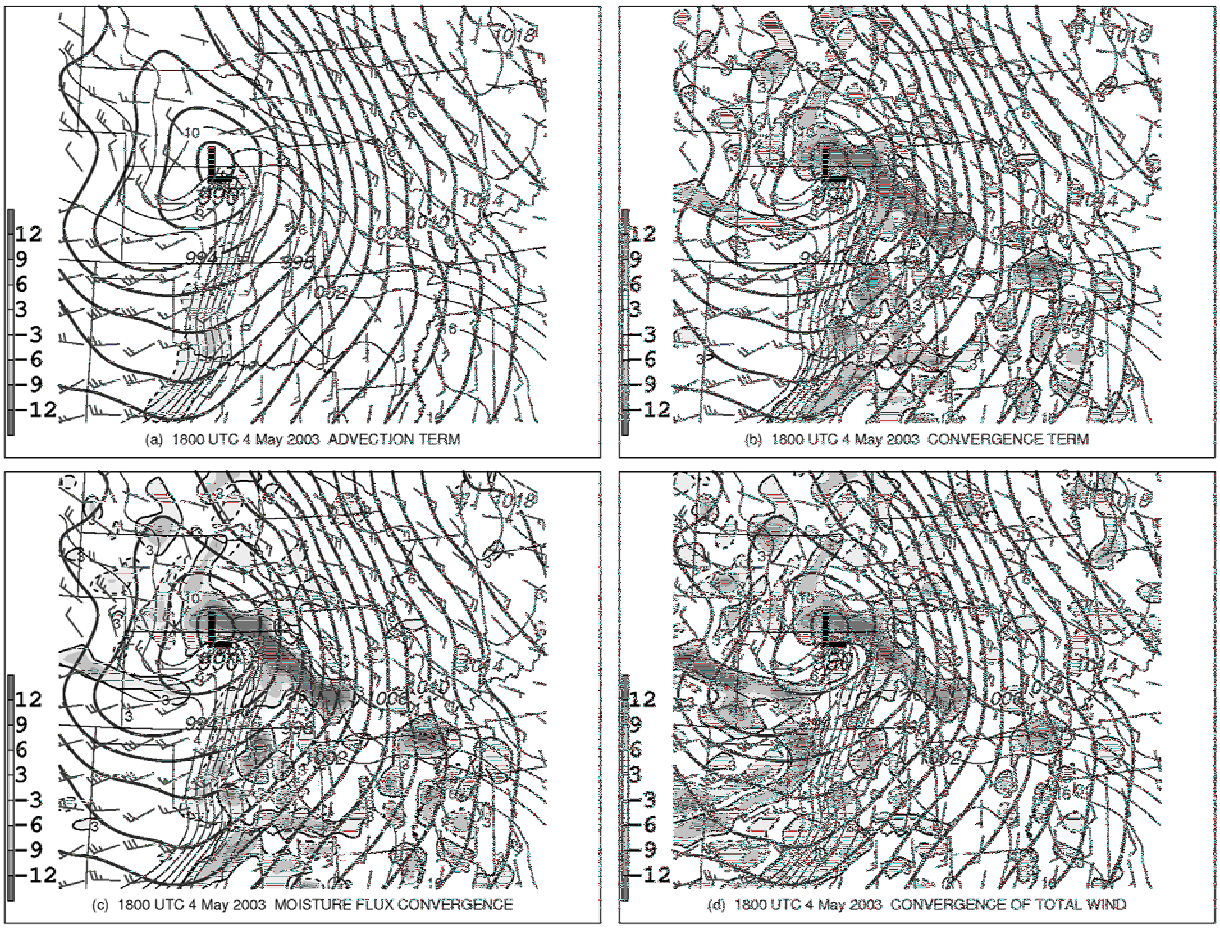

Fig. 1 Surface objective analysis valid at 1800 UTC on 4 May 2003. Sea-level pressure (thick solid lines every 2 mb), specific humidity (thin solid lines every 2 g kg^{-1}). Shaded regions represent (a) the advection term in MFC expression (10^{-4} g kg^{-1} s^{-1}), where positive values represent moist advection, (b) the convergence term in MFC expression (10^{-4} g kg^{-1} s^{-1}), where positive values represent convergence, (c) the total moisture flux convergence (10^{-4} g kg^{-1} s^{-1}), where positive values represent positive MFC, and (d) the horizontal mass convergence of the total wind ($10^{-5}s^{-1}$), where negative values represent horizontal mass divergence. Thin dashed lines (thin solid lines) delineate negative (positive) values associated with shaded regions for

each panel. Pennant, barb, and half-barb represent wind speeds of 25, 5, and 2.5 m s^{-1}, respectively.

Fig. 2 Schematic of subcloud horizontal mass convergence (conv) as it relates to cumulus convection (represented by cloud outline). Arrows represent streamlines. Thick dashed line indicates top of PBL. (a) Surface horizontal mass convergence maximum is associated with a deep tropospheric circulation and deep moist convection. (b) Surface horizontal mass convergence maximum is associated with shallow cumulus development owing to midlevel subsidence and/or a capping inversion. (c) Surface horizontal mass convergence maximum is

located near change in boundary layer depth. Thin dashed line indicates isentropic surfaces. (d) Horizontal mass convergence maximum is rooted above the local boundary layer.

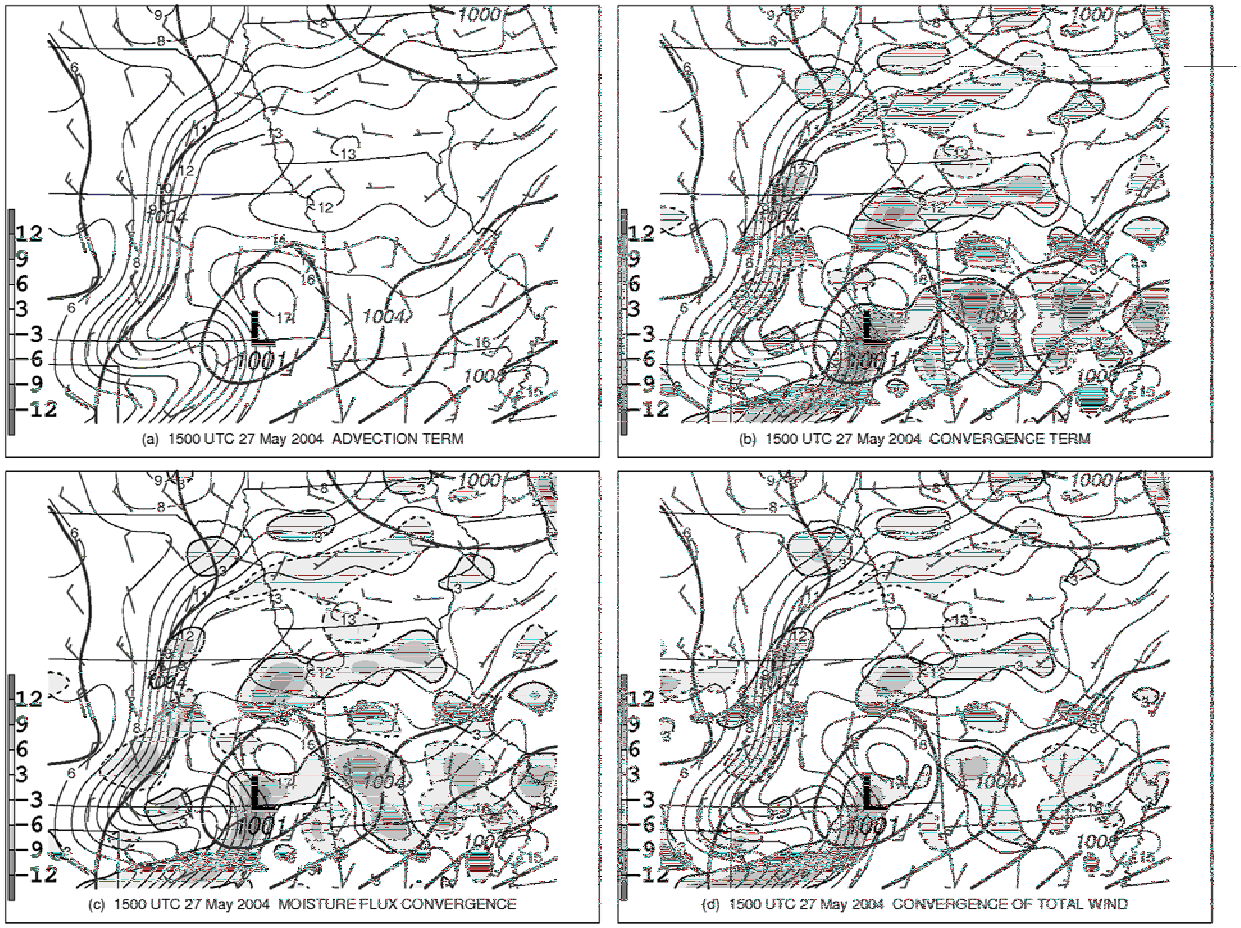

Fig. 3 As in Fig. 1, except for 1500 UTC on 27 May 2004, and specific humidity contour interval is 1 g kg^{-1}.

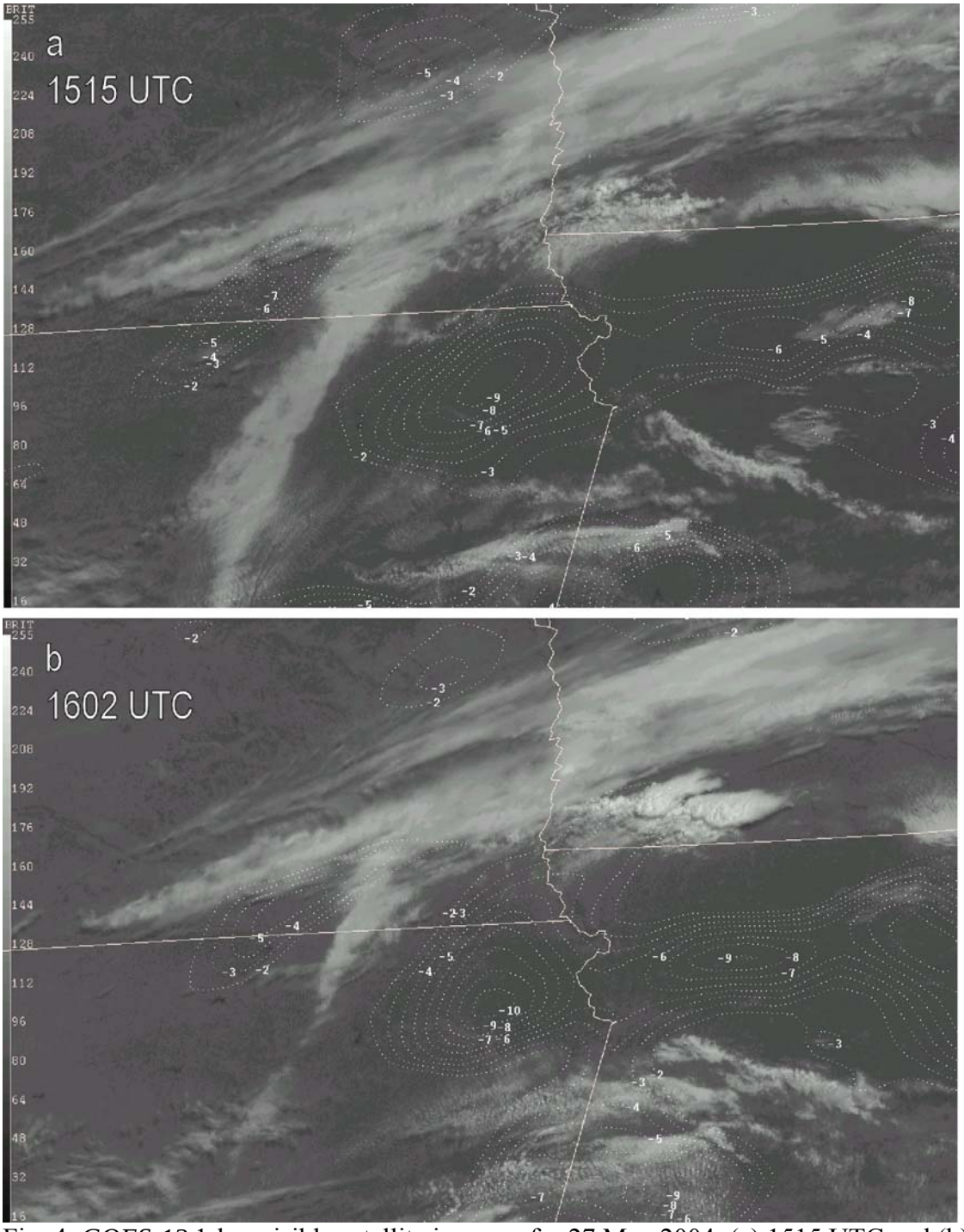

Fig. 4 *GOES-12* 1-km visible satellite imagery for 27 May 2004: (a) 1515 UTC and (b) 1602 UTC. Surface moisture flux convergence (dotted lines, 10^{-4} g kg^{-1} s^{-1}, negative values only) from SPC surface objective analysis (Bothwell et al. 2002) at (a) 1500 UTC and (b) 1600 UTC.

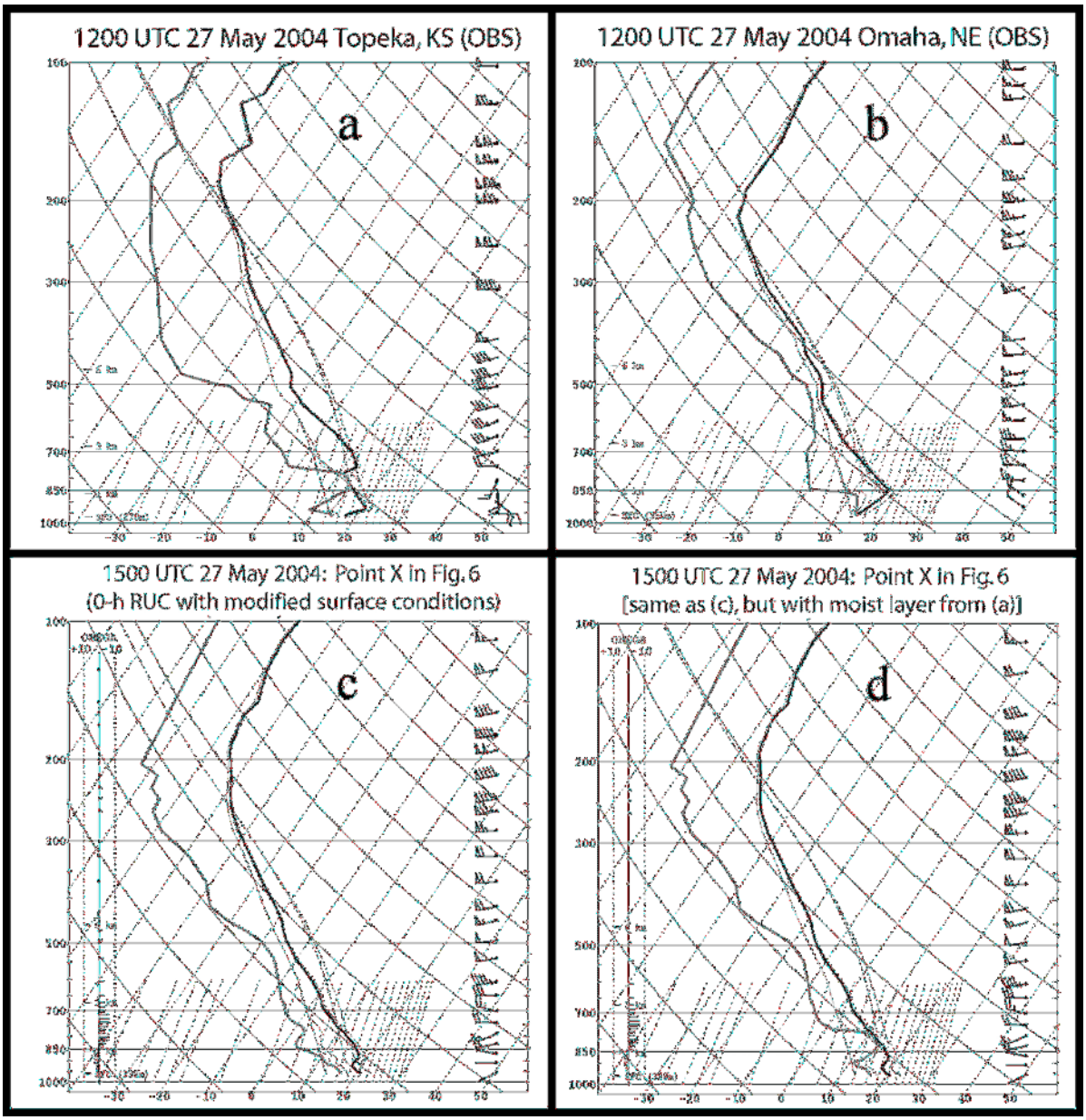

Fig. 5 Skew *T*–log *p* plots of observed temperature (dark gray lines) and dewpoint temperature (light gray lines) for 1200 UTC 27 May 2004: (a) Topeka, KS, and (b) Omaha, NE. (c) RUC 0-h forecast sounding with modified surface conditions valid 1500 UTC 27 May 2004 near the Missouri/Iowa border (see "X" in Fig. 6 for location). (d) As in (c), except sounding is modified using low-level moist layer found on 1200 UTC Topeka sounding in (a). Horizontal bars represent vertical distribution of vertical motion ($\mu b\ s^{-1}$). Pennant, barb, and half-barb represent wind speeds of 25, 5, and 2.5 m s^{-1}, respectively.

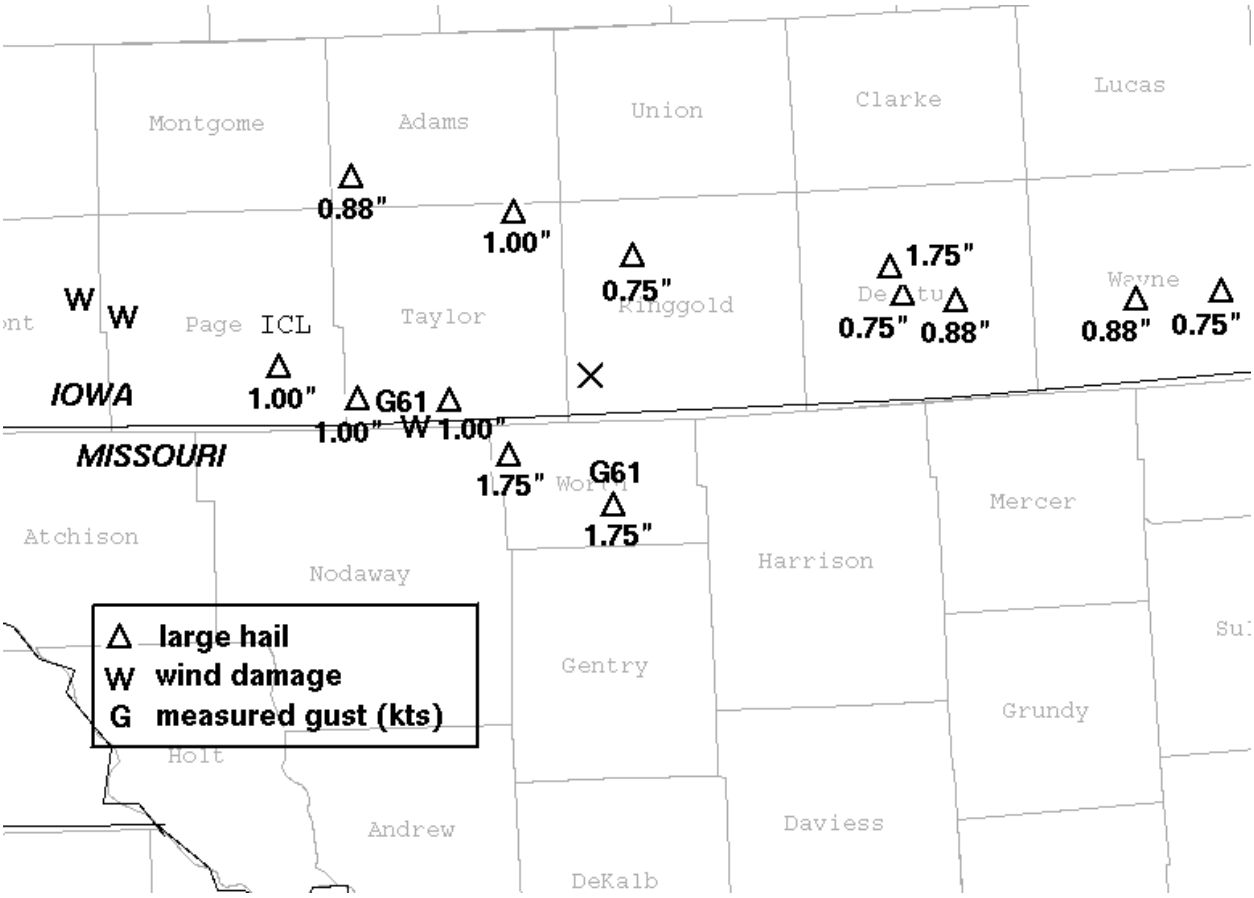

Fig. 6 Preliminary National Weather Service storm report data for 1600–1900 UTC 27 May 2004 across northern Missouri and southern Iowa. Location of RUC sounding in Fig. 5c,d is denoted by "X" in southwestern Ringgold County, Iowa. Clarinda, Iowa is denoted by ICL. County borders are indicated by the gray lines with county names listed within.